



Exploring the role of soil geochemistry on Mn and Ca uptake on 75-year-old mine spoils in western Massachusetts, USA

Jonah Jordan · Richard S. Cernak Sr. · Justin B. Richardson 

Received: 16 January 2019 / Accepted: 22 May 2019
© Springer Nature B.V. 2019

Abstract Manganese pollution to plants, soils, and streams from Mn-rich mine spoils is a global and persistent issue. Some former mining sites can be revegetated readily while others struggle to support plants. We explored Mn in plants and soils following 75 years of soil development and reforestation of a pine-northern hardwood forest at the former Betts Mine in western Massachusetts, USA. We studied soils on four Mn-rich mine spoils and at two control sites: an undisturbed location adjacent to the mine and on a non-Mn mineral bearing rock formation to determine if soil conditions have influenced the uptake of Mn and Ca by vegetation. We collected mid-season foliage from five dominant canopy trees and four common understory plants and excavated three soil pits at each site during July 2018. We found that control sites had lower total Mn ($980 \pm 140 \mu\text{g g}^{-1}$) in their soils than on the mine spoil sites ($5580 \pm 2050 \mu\text{g g}^{-1}$). Our soil data indicated that $< 1\%$ of total Mn was strong acid extractable at mine spoil soils and control sites. Surprisingly, the canopy trees established on mine spoils at the Betts Mine had equal to or lower foliar Mn concentrations

($840 \pm 149 \mu\text{g g}^{-1}$) and lower Mn/Ca ratios ($0.3 \pm 0.1 \text{ mol mol}^{-1}$) than at control sites ($1667 \pm 270 \mu\text{g g}^{-1}$; $1.1 \pm 0.2 \text{ mol mol}^{-1}$), refuting our hypothesis of mine spoils driving highest Mn uptake. Soil pH and physicochemical properties suggest Mn primarily exists within primary minerals or form insoluble oxides at the mine spoil sites. Our results suggest higher Ca availability and pH in soils likely reduced Mn uptake and promoted reforestation of the mine spoils.

Keywords Biogeochemistry · Phytotoxicity · Mn toxicity · Mn/Ca ratio

Introduction

Manganese (Mn) is an essential element for modern society, as part of batteries, chemical reagents, and fertilizers; with a 2010 estimate of the global Mn ore production to be 44.1 million metric tons (Kabata-Pendias and Mukherjee 2007; Westfall et al. 2016). Manganese is a ubiquitous metal, making up 0.10% of the Earth's crust, and is present as oxides, carbonates and silicates (Krauskopf 1979; Adriano 2001). The extraction of Mn is concentrated in Australia, Brazil, South Africa and Gabon (Adriano 2001), while smelting is distributed across Asia, Africa, Australia, and Europe (Westfall et al. 2016). Environmental

J. Jordan
Department of Environmental Studies, College of Idaho,
Caldwell, ID 83605, USA

J. Jordan · R. S. Cernak Sr. · J. B. Richardson (✉)
Department of Geosciences, University of Massachusetts,
611 North Pleasant Street, Amherst, MA 01003, USA
e-mail: Jbrichardson@umass.edu

impacts from Mn extraction and production are generally tied to handling of raw materials, which include overburden, spoils, and tailings which remain at the site. Impacts from Mn released during the Mn extraction and production process to the environment range from fish die-offs (Stubblefield et al. 1997) and toxicity to plants (Kreutzer 1972; Clair and Lynch 2005).

Dealing with subsequent issues from Mn extraction, mine spoils and tailings can be difficult, partly due to issues with establishing or maintaining cover vegetation. Mine spoils and tailings are often toxic to plants because of acidity from pyrite oxidation or exposure to toxic concentrations of Mn or other elements such as Cd and Zn. Although many Mn mines can produce acid mine drainage (AMD), other Mn mine spoils frequently have slightly acid to basic conditions; Yang et al. (2014) observed soil pH to be between 5.3 to 6.6 and Juárez-Santillán et al. (2010) observed pH to be between 7.7 to 8.2 in Mn mine spoils. In these soils with lower pH, phytotoxicity can occur due to elevated concentrations of Mn and other elements like Cd, Cr, Pb, and Zn (Li and Yang 2008; Yang et al. 2014). As a prime example, the Huayan Mn mine spoils have toxic concentrations of Mn as well as accessory elements like Cd, Pb, and Zn and are primarily covered with only grasses (Yang et al. 2014). Moreover, Yang et al. (2014) found that only grass could be supported on the Mn-rich mine tailings instead of the native subtropical forest species. The Mn toxicity can persist for decades even with remediation efforts, leading to potentially hazardous concentrations to wildlife and humans in the foliar tissues (Li et al. 2007). Establishment of vegetation can promote the retention of Mn in mine spoils by reducing the downward leaching during the growing season (Herndon et al. 2019).

Because of the relatively high pH, the mode of toxicity to plants on Mn mine spoils is unclear; Mn primarily exists as insoluble secondary oxides under typical oxic, slightly acid to basic soils (Millaleo et al. 2010). One hypothesis is that Mn phytotoxicity may be controlled by available concentrations instead of total Mn concentrations (Millaleo et al. 2010). Bioavailability may be an important factor because immobilized forms are more difficult for extraction and uptake by plant roots. However, both the grass-dominated mine spoils in Yang et al. (2014) in a subtropical region of China and the plant covered ecosystem

Juárez-Santillán et al. (2010) in temperate region of Mexico observed < 1% of Mn in mine spoils to be bioavailable. Another hypothesis is that the plant communities in Juárez-Santillán et al. (2010) site is dominated with Mn-tolerant plants. Manganese toxicity in plants generally occurs when foliar concentrations exceed $500 \mu\text{g g}^{-1}$, but some plants (such as Mn-hyperaccumulators) can exceed $2000 \mu\text{g g}^{-1}$ without showing signs of phytotoxicity (Adriano 2001; Kraepiel et al. 2015). Further, some perennial herbaceous and woody plants can hyperaccumulate Mn concentrations in foliage between 14,000 to 32,000 mg kg^{-1} in their tissues (e.g., Xue et al. 2004; Pollard et al. 2009). We hypothesize that the presence of other mineral nutrient elements in Mn mine spoils may be just as important as the plant species, not just for phytotoxicity but also ameliorating toxicity. Manganese toxicity may be mediated by the abundance of Ca (see Watmough et al. 2007; Richardson 2017). One of the main toxic effects of Mn on plants is the interference of Mn with Ca chemical signaling (Da Silva and Williams 2001) and higher abundance of Ca can help prevent phytotoxicity issues (Robson and Loneragan 1970; Millaleo et al. 2010).

The objective of this study was to assess foliar and soil Mn concentrations in a pine-northern hardwood forest established upon mine spoils at the Betts Mine in western Massachusetts and if soil pH and Ca abundance are influencing Mn uptake. The overburden and spoils were left in four distinct piles around the mine site and have become revegetated over 75 years following the ceasing of operations in 1943. The first goal of this study was to determine if Mn concentrations were elevated in the northern hardwoods or if their mineral nutrition with respect to Ca influences their uptake when compared to control sites. Second, we aimed to determine if soil conditions influenced the uptake of Mn by the vegetation when compared to control sites. We hypothesized that the soils developed from the mine spoils of the Betts Mine would have higher Mn concentrations than at nearby control sites but high concentrations of Ca allow the northern hardwoods to avoid excessive Mn uptake. Furthermore, we predicted low bioavailability of Mn due to Mn remaining in silicates or precipitating as Mn oxides.

Materials and methods

Geologic setting and history of the Betts Mine

We studied the former Betts Mine located immediately north of the boundary with West Cummington in the town of Plainfield, Massachusetts, USA (Fig. 1). The former Betts Mine is in the Hawley Formation, a sequence of lower Paleozoic units on the eastern flank of the Berkshire Mountains. The Hawley formation consists of deformed and polymetamorphosed shale, graywacke and volcanic rocks (Hickmott 1982; Hickmott et al. 1983). The Betts Mine occurred within a carbonaceous metasedimentary unit of the Hawley formation, consisting of quartz–muscovite–biotite–garnet–chlorite phyllite and fine-grained quartzite interbedded with feldspathic schist and bands of amphibolite. The petrologic studies by Hickmott et al. (1983) demonstrate that the rocks have undergone two phases of deformation and two periods of metamorphism. Further details about the petrology

can be found in Hickmott (1982) and Hickmott et al. (1983). Extraction of low-grade Mn-carbonate ore as well as gem-grade rhodonite began at the Betts deposit in 1848. Mining operations of the two open pits peaked during the early 1940s but decreased and continued stochastically afterward (Hickmott et al. 1983; Quinn 1945). Total production was between 10,000 to 12,000 tons of ore, which averaged 20 to 25% Mn (Quinn 1945). The Mn ore was not processed via smelting or other similar techniques at the Betts mine, but moved by truck for processing elsewhere. The principal Mn-bearing minerals found in the mine spoils are rhodonite ($MnSiO_3$), rhodochrosite ($MnCO_3$), spessartine ($Mn_3Al_2(SiO_4)_3$), kutnohorite ($Ca, (Mn, Mg, Fe)(CO_3)_2$), tephroite (Mn_2SiO_4), and sonolite ($Mn_9(SiO_4)_4(OH)_2$) (Quinn 1945; Hickmott et al. 1983).

There are four distinct spoil piles varying in amount of spoils, overburden, and fill soil. The four zones have varying compositions of overburden and mine spoils and have been named Zones A, B, C, and D (Fig. 1, Table 1). Zones A and C are predominately mine spoils varying in 1–9 m in depth, with rock fragments varying from gravel to boulders (Table 1). Zone B is a mixture of large boulder spoils and overburden. Zone D is a mix of overburden, spoils and added soil (Table 1). Below the mine spoils in Zone B and D is glacial-till, which was deposited during the retreat of the Laurentian ice sheet in the Wisconsin glacialiation ~ 14,000 years ago. Control mine site was located ~ 80 m away from the mine spoils, in a minimally disturbed mature oak-maple forest that was not impacted from mining operations. The control river site was located 2.3 km away in secondary regrowth forest that had been cleared for pasture until the late 1890s (Fig. 1, Table 1). The control river site was set upon quartz–muscovite–feldspar–garnet schists of the Goshen formation and was not known to have any rhodochrosite or rhodonite bearing rocks. Furthermore, it was off of the metal-rich Hawley formation. We selected the control river site to represent the species present in a disturbed, secondary regrowth forest while avoiding Mn-rich underlying bedrock.

Soil and rock sampling mine spoils and control sites

Three soil pits were excavated at each mine spoil and control site during July 2018. The soil pits locations were chosen across features of the landscape to

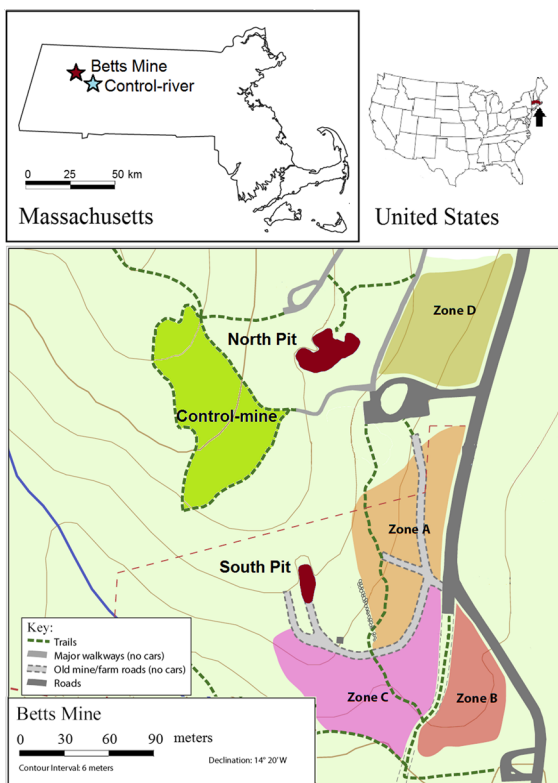


Fig. 1 Location of Betts Mine sampling locations (Zones A, B, C, and D) and the two control areas (control mine and control river)

Table 1 Location of study areas and descriptions of vegetation present

Site	Latitude	Longitude	Elevation (m)	Parent material	Canopy trees studied [†]	Understory plants studied [‡]
Zone A	42.496°N	– 72.946°W	431	Mine spoils	A, B, C, E	A, B, D
Zone B	42.496°N	– 72.946°W	427	Mine spoils	A, B, C, D, E	A, B, C, D
Zone C	42.496°N	– 72.946°W	431	Mine spoils	A, B, C, D,	A, B, C, D
Zone D	42.496°N	– 72.946°W	436	Mine spoils Overburden	A, C, D	A, B, D
Control mine	42.497° N	– 72.947° W	450	Glacial-till	C, E	A, B, D
Control river	42.505° N	– 72.919° W	392	Glacial-till	C, D, E	A, B, C, D

[†] A *Betula lenta* (black birch), B *Betula papyrifera* (paper birch), C *Acer saccharum* (sugar maple), D *Fraxinus pennsylvanica* (green ash), E *Fagus grandifolia* (American beech)

[‡] A *Acer penslyanicum* (striped maple), B *Maianthemum racemosum* (false Solomon's seal), C *Onoclea sensibilis* (Sensitive fern), D *Polystichum acrostichoides* (Christmas fern)

capture the maximum variation in soils and mine spoils. First, 15 × 15 cm square sections of organic horizons were separated from the underlying mineral soil and collected. Second, a soil pit was excavated to 1 m depth or lithic contact and sampled by each master horizon. The rock fraction was visually estimated as a percent surface area of the horizon of the soil pit face. Representative rock hand samples (5–30 cm in diameter) were collected from throughout the soil pit. To determine soil bulk density, a cylindrical steel core (10.5 cm length, 7.3 cm diameter) was collected from the face of each soil horizon. Soil horizons with rock fragments greater than 5 cm in length could not be sampled for bulk density using the core. Soils samples were weighed, air-dried at 25 °C to a constant mass, sieved to < 2 mm, and roots > 5 mm in diameter were removed. Organic horizon masses were calculated using oven-dried subsamples.

Soil physicochemical analyses

Soil pH, texture, and %organic matter were measured for each soil horizon (Table 2). For soil pH, a 2:5 soil–CaCl₂ solution (5 g soil to 12.5 g 0.1 M CaCl₂) was used to determine soil pH. The CaCl₂ slurries were shaken for 1 h using a wrist-action shaker and vacuum extracted through a Whatman 40 filter. The pH of the extract was measured with a pH meter (8015 VWR). Loss-on-ignition was used to estimate % SOM, which is a simple and qualitative method but may overestimate organic matter content due to mineral dehydration and carbonates (Santisteban et al. 2004). To

determine the percent loss-on-ignition, a 4-g air-dried subsample was combusted at 550 °C for 6 h. Soil texture was quantified using a modified Bouyoucos method with hydrometer readings taken at 60 s and 1.5 h after complete mixing of standard 1 L graduated columns (Gee and Bauder 1985; Richardson et al. 2013).

Plant foliage sampling

Mid-season foliage samples were collected from five dominant canopy trees: *Acer saccharum*, *Betula lenta*, *Betula papyrifera*, *Fraxinus pennsylvanica*, and *Fagus grandifolia* as well as four common understory plants: *Acer penslyanicum*, *Maianthemum racemosum*, *Onoclea sensibilis*, and *Polystichum acrostichoides* in triplicate from each site in early July 2018 (Table 1). Additional trees present but not sampled due to limited distribution across sites were *Pinus strobus*, *Tsuga canadensis*, and *Quercus rubra*. Foliage was collected from branches in the upper canopy 16 to 24 m above the ground by branch-downing using weighted ball attached to nylon throwline. Tree DBH was measured and leaves were visually inspected for disease, damage, or senescence. Understory plants were collected using stainless-steel clippers. Foliage samples were air-dried at 30 °C in paper bags in a greenhouse for 2 weeks. Foliage samples were not washed to remove dust as it could leach elements from within the plant tissues.

Table 2 Average soil properties at the four study areas of mine spoils at the Betts Mn Mine plus an undisturbed control adjacent to the mine and another control off the mineral-rich Rowe–Hawley formation

Dominant vegetation type	N	Horizon	Depth interval (cm)	%LOI (%)	PH	%Clay (%)	%Silt (%)	%Sand (%)
Control mine	3	A	0–9	13 ± 2	3.7 ± 0.2	9 ± 1	14 ± 1	77 ± 2
	3	B	9–35	5 ± 1	4.3 ± 0.1	2 ± 1	19 ± 2	79 ± 3
	3	BC	35–75	4 ± 1	4.5 ± 0.1	4 ± 2	24 ± 3	73 ± 5
Control river	3	A	0–12	17 ± 1	3.6 ± 0.2	11 ± 2	17 ± 4	72 ± 2
	3	B1	12–24	7 ± 1	4.4 ± 0.1	3 ± 1	20 ± 1	77 ± 1
	3	B2	24–40	5 ± 1	4.5 ± 0.1	5 ± 3	30 ± 4	65 ± 5
	3	BC	40–60	5 ± 1	4.7 ± 0.2	2 ± 1	26 ± 3	72 ± 3
Zone A	3	A	0–17	8 ± 1	5.2 ± 0.4	4 ± 2	9 ± 5	87 ± 6
	3	B1	17–34	3 ± 1	5.2 ± 0.5	3 ± 3	12 ± 4	85 ± 6
	3	B2	34–53	3 ± 1	5.0 ± 0.4	3 ± 2	34 ± 16	63 ± 16
	3	BC	53–79	4 ± 1	5.2 ± 0.4	4 ± 2	23 ± 5	73 ± 4
Zone B	3	A	0–9	16 ± 1	4.6 ± 0.5	5 ± 3	16 ± 4	78 ± 7
	3	B1	9–23	7 ± 1	4.5 ± 0.1	2 ± 2	17 ± 1	81 ± 1
	3	B2	23–45	4 ± 1	4.6 ± 0.1	2 ± 2	19 ± 3	78 ± 5
	3	BC	45–69	3 ± 1	4.8 ± 0.2	1 ± 1	18 ± 1	81 ± 2
Zone C	3	A	0–29	6 ± 2	5.9 ± 0.6	6 ± 3	10 ± 3	83 ± 1
	3	AB	29–66	7 ± 2	5.3 ± 0.7	6 ± 3	7 ± 1	87 ± 2
	3	BC	66–86	4 ± 1	5.2 ± 0.7	4 ± 2	18 ± 5	78 ± 7
Zone D	3	A	0–10	10 ± 3	5.2 ± 0.3	4 ± 1	14 ± 2	82 ± 2
	3	B1	10–30	5 ± 1	4.8 ± 0.5	2 ± 1	16 ± 1	82 ± 2
	3	B2	30–53	3 ± 1	4.9 ± 0.3	1 ± 1	16 ± 2	83 ± 4
	3	BC	53–84	3 ± 1	4.9 ± 0.2	1 ± 1	21 ± 3	79 ± 3

Mean values are given ± 1 standard error

Soil extraction and total foliage digestions

A strong acid digestion following USEPA method 3051A was used to quantify extractable Ca, Mn, and Fe concentrations through open vessel digestion (Table 3). Strong acid digestion was used instead of other operationally defined methods to measure all non-primary silicate mineral lattice metals that may become dissolved or biologically relevant over decades to centuries (Chen and Ma 1998). This method can dissolve metals within organic matter, secondary oxides, and poorly crystalline secondary minerals that undergo dissolution below pH 1. However, primary silicate minerals, such as quartz and feldspars, are not dissolved, but edges on mineral surfaces can be corroded (Chen and Ma 1998). The digestion process used 1.0 g (± 0.1 g) of soil samples, digested with 5 mL of 9:1 ratio of trace metal grade nitric acid to hydrochloric acid (15 M HNO₃ + 10 M

HCl, Fisher Scientific). The solution was heated to 80 °C for 45 min using a hot plate and diluted to 50 mL using 18.2 MΩ cm deionized water. For every 20 samples, a preparation blank and duplicate sample were included. Samples were analyzed on a Shimadzu 2030 Inductively Coupled Plasma-Mass Spectrometer (Shimadzu Scientific Instruments, Columbia, Maryland). Calcium, Mn, and Fe concentrations in the preparation blank were < 0.1% of their respective measured concentrations and all duplicates were within 12% CV. NIST Montana Soil 2711b standard reference material was also digested following this protocol and recoveries were between 83–97% of their certified values.

Foliage samples were analyzed for trace element analyses using a total digestion. For the digestion, 0.50 g (± 0.05 g) of crushed, dry plant samples were ashed at 550 °C for 6 h. At least three leaves were used for each analysis and midveins were removed to

Table 3 Concentrations of extractable, total, and % extractable Ca, Fe, and Mn averaged across soil pits and soil horizons for each study area

	N	Horizon ($\mu\text{g g}^{-1}$)	Ca EXT ($\mu\text{g g}^{-1}$)	Fe EXT ($\mu\text{g g}^{-1}$)	Mn EXT ($\mu\text{g g}^{-1}$)	%Ca EXT (%)	%Fe EXT (%)	%Mn EXT (%)
Control at mine	3	A	11 \pm 7	101 \pm 48	9 \pm 1	0.2	0.3	0.7
	3	B	2 \pm 1	18 \pm 7	9 \pm 4	0.0	0.0	0.5
	3	BC	5 \pm 1	5 \pm 2	3 \pm 1	0.0	0.0	0.3
Control river	3	A	12 \pm 6	86 \pm 26	3 \pm 1	0.3	0.2	0.4
	3	B1	5 \pm 2	51 \pm 22	4 \pm 1	0.1	0.1	0.5
	3	B2	6 \pm 2	11 \pm 3	4 \pm 1	0.1	0.0	0.5
	3	BC	12 \pm 5	7 \pm 4	3 \pm 1	0.2	0.0	0.4
Zone A	3	A	240 \pm 51	130 \pm 74	88 \pm 3	2.7	0.3	1.2
	3	B1	94 \pm 41	3 \pm 1	18 \pm 6	0.9	0.0	0.4
	3	B2	63 \pm 43	9 \pm 5	12 \pm 5	0.6	0.0	0.5
	3	BC	158 \pm 70	11 \pm 7	48 \pm 22	1.5	0.0	0.8
Zone B	3	A	134 \pm 103	62 \pm 21	33 \pm 11	1.9	0.1	1.0
	3	B1	12 \pm 10	59 \pm 26	8 \pm 3	0.3	0.1	0.9
	3	B2	6 \pm 4	9 \pm 3	2 \pm 1	0.1	0.0	0.2
	3	BC	18 \pm 8	27 \pm 25	5 \pm 2	0.2	0.1	0.4
Zone C	3	A	381 \pm 169	119 \pm 92	115 \pm 37	4.7	0.2	0.5
	3	AB	227 \pm 172	201 \pm 63	175 \pm 47	2.5	0.3	0.6
	3	BC	270 \pm 105	23 \pm 7	55 \pm 15	3.5	0.0	2.8
Zone D	3	A	239 \pm 88	38 \pm 15	29 \pm 7	2.5	0.1	0.8
	3	B1	53 \pm 41	109 \pm 73	11 \pm 7	0.5	0.2	0.6
	3	B2	31 \pm 19	55 \pm 22	17 \pm 4	0.4	0.1	0.5
	3	BC	25 \pm 16	4 \pm 1	8 \pm 3	0.3	0.0	0.2

Mean values are given \pm 1 standard error

avoid dilution by woody material which generally have much lower concentrations of elements (e.g., Richardson and Friedland 2016). Foliage was not washed as it could leach out Mn or other elements. Every 20 samples included one digestion blank and one duplicate. The ashes were digested with 5 mL of 9:1 ratio of trace metal grade nitric acid to hydrochloric acid (15 M HNO₃ + 10 M HCl, Fisher Scientific). The solution was heated to 80 °C for 45 min using a hot plate. Calcium, Mn, and Fe concentrations in the preparation blank were < 0.1% of their respective measured concentrations and all duplicates were within 6% CV. NIST Peach Leaf 1354 standard reference material was also digested following this protocol and recoveries were 87–94% of the certified values.

Total soil and mineral XRF and XRD analyses

Total concentrations of Ca, Mn, and Fe in soils (Table 4) and rocks (Table 5) were determined using a X-200 XRF instrument from SciAps (SciAps Inc., Woburn, MA). The X-200 utilizes three energy beams: 40 kV, 10 kV, and 50 kV, from an Rh anode alloy. For a detector, it uses a 20-mm two silicon drift detector and 135 eV resolution FWHM at 5.95 Mn K-alpha line. Spectra were analyzed using Compton Normalization (EPA Method 6200) and calibrated with data for USGS rock standards for elemental concentrations. Prior to sample analysis, an internal instrument calibration and external USGS Hawaiian basalt standard reference material (BHVO-2) was performed. For the USGS Hawaiian basalt BHVO-2, Ca, Mn, and Fe concentrations were within 4% of its certified values. Soil samples were crushed to < 0.05 mm and

Table 4 Total Ca, Fe, and Mn concentrations averaged across soil pits and soil horizons for each study area using XRF

	<i>N</i>	Horizon ($\mu\text{g g}^{-1}$)	Ca total ($\mu\text{g g}^{-1}$)	Fe total ($\mu\text{g g}^{-1}$)	Mn total ($\mu\text{g g}^{-1}$)
Control at mine	3	A	5900 ± 320	41,600 ± 3800	1450 ± 440
	3	B	6580 ± 370	42,000 ± 2400	1300 ± 320
	3	BC	8170 ± 720	40,400 ± 1600	1140 ± 240
Control river	3	A	4970 ± 530	42,300 ± 1000	620 ± 40
	3	B1	6180 ± 1070	43,000 ± 2100	710 ± 20
	3	B2	6060 ± 880	42,500 ± 1200	780 ± 140
	3	BC	6840 ± 330	41,900 ± 1000	740 ± 40
Zone A	3	A	9030 ± 1930	52,200 ± 3800	7960 ± 1540
	3	B1	8720 ± 2110	52,900 ± 5800	7610 ± 3050
	3	B2	10,090 ± 530	50,400 ± 3500	2300 ± 470
	3	BC	9800 ± 650	51,700 ± 2300	5400 ± 1860
Zone B	3	A	6080 ± 860	44,600 ± 2000	2860 ± 1720
	3	B1	4980 ± 330	43,700 ± 1200	810 ± 80
	3	B2	7200 ± 1020	47,800 ± 2500	1020 ± 60
	3	BC	7920 ± 1390	46,600 ± 3300	1420 ± 110
Zone C	3	A	8020 ± 5590	68,600 ± 6500	20,110 ± 7900
	3	AB	8970 ± 620	70,700 ± 8600	23,060 ± 8880
	3	BC	7370 ± 250	51,600 ± 1300	1530 ± 250
Zone D	3	A	8850 ± 1620	48,100 ± 2200	3490 ± 840
	3	B1	7770 ± 1740	48,200 ± 700	1660 ± 257
	3	B2	7820 ± 1040	48,100 ± 2700	2700 ± 1360
	3	BC	8640 ± 970	50,300 ± 3800	3240 ± 1770

Mean values are given ± 1 standard error

Table 5 Total Ca, Fe, and Mn concentrations in mine spoil rocks and minerals (> 5 cm diameter) collected from within soil profiles in Zones A, B, C, and D

	<i>N</i>	Ca total ($\mu\text{g g}^{-1}$)	Fe total ($\mu\text{g g}^{-1}$)	Mn total ($\mu\text{g g}^{-1}$)
<i>Minerals</i>				
Rhodonite/Spessartine-rich rock samples	7	22,857 ± 758	42,262 ± 402	59,484 ± 595
Rhodochrosite/kutnohorite-rich rock samples	6	23,207 ± 449	39,935 ± 450	221,662 ± 1312
<i>Rocks</i>				
Micaceous schist	12	15,938 ± 67	82,726 ± 503	27,054 ± 416
Amphibolite	12	4707 ± 353	82,301 ± 594	2882 ± 136
Feldspathic schist	15	4175 ± 152	8186 ± 223	363 ± 64
Quartzite	14	840 ± 242	< 10	< 10

Rock samples were identified as hand samples and minerals were determined using XRD. Mean values are given ± 1 standard error

packed into 7 mL polypropylene tube lined with 6 μm thick polyethylene terephthalate sheet. All samples were analyzed using the soil analysis mode and analyzed for 130 s per sample.

Soil and rock subsamples were processed to determine bulk mineralogy. First, samples were ground to < 0.05 mm and treated with 30% (w/w)

H_2O_2 to remove organic matter and washed with four cycles of DI water shaking, centrifuging, and decanting. The mineralogy of rock and soil samples was determined qualitatively using X-ray diffraction (XRD). Crushed samples fixed onto glass slides and scanned with CuK α radiation (15 mA, 40 kV) using a Rigaku Miniflex 600 (Rigaku Analytical Devices,

Wilmington, Massachusetts) using a step size of 2° per min at 0.025 steps from 10° to 70° . The Rigaku Miniflex 600 was equipped with a graphite monochromator and a D/teX Ultra silicon strip detector. Minerals were identified using the Crystallography Open Database of mineral standards XRD pattern library (Grazulis et al. 2009).

Descriptive and statistical analyses

For soil comparisons, the three soil pits for each site were grouped together for each master soil horizon and again with all soil horizons together. In the foliar comparisons, data were grouped together either by species or site. Descriptive statistics were calculated in MATLAB. In text, mean values are given ± 1 standard error. For comparing foliar concentrations and across sites, the parametric *t* test and ANOVA were used. Data were tested for normal distribution using the Lilliefors test (Lilliefors 1967) and logarithmically or exponentially transformed when necessary to establish normality. Due to the limited sample sizes when comparing among soil pits horizons, nonparametric statistical tests were used: rank-sign test and Kruskal–Wallis test.

Results and discussion

Extractable and total Ca, Mn, and Fe soil concentrations

Our investigation of mine spoil mineralogy shows the Mn ore extraction process was effective, as rhodochrosite and kutnohorite were found in only a few hand-sized rocks (Fig. 2). We observed two types of Mn-rich rocks, rhodonite–spessartine-dominated rocks and rhodochrosite–kutnohorite-dominated rocks (Fig. 2), with higher Mn concentrations in the rhodochrosite–kutnohorite-dominated rocks (Table 5). Rhodonite was present in more soil samples than rhodochrosite and kutnohorite. The soil XRD patterns demonstrate that the mineralogy was primarily quartz, feldspars (albite and anorthite), and micas (both biotite and muscovite) with minor constituents of garnets (specifically spessartine and almandine), other clay minerals (vermiculite and kaolinite), calcite and kutnohorite, and birnessite (Fig. 3). Important differences were the presence of rhodonite,

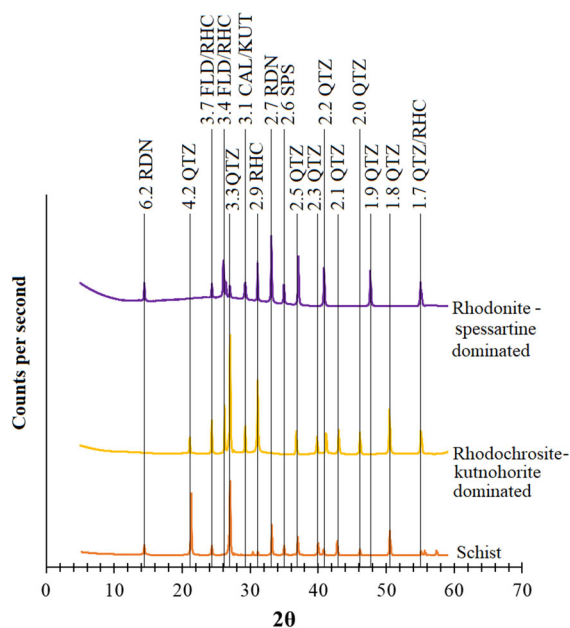


Fig. 2 Representative hand-sample size rock fragment x-ray diffraction (XRD) patterns. Values indicated are d-spacings and abbreviations are for the following minerals *QTZ* quartz, *RHC* rhodochrosite, *FLD* feldspar, *KUT* kutnohorite, *CAL* calcite, *RDN* rhodonite, *SPS* spessartine

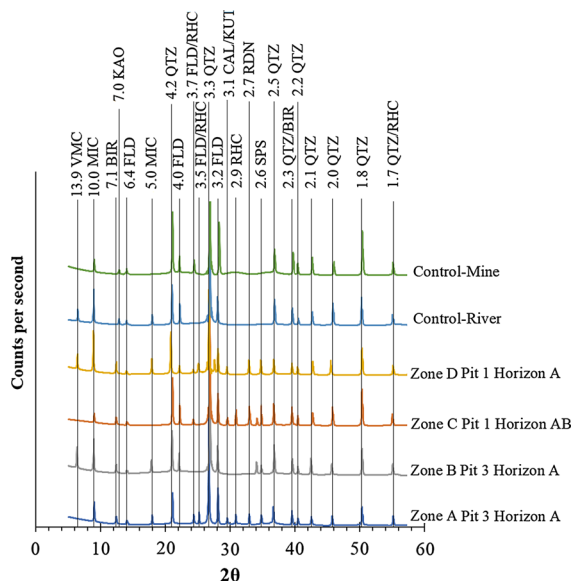


Fig. 3 Representative A horizon x-ray diffraction (XRD) patterns across the four mine spoil zones and two control sites. Values indicated are d-spacings and abbreviations are for the following minerals *QTZ* quartz, *RHC* rhodochrosite, *FLD* feldspar, *KUT* kutnohorite, *CAL* calcite, *RDN* rhodonite, *SPS* spessartine, *VMC* vermiculite, *MIC* micas, *BIR* birnessite, *KAO* kaolinite

rhodochrosite, calcite and kutnohorite, birnessite, and spessartine in soils formed from mine spoils and absence in the control soils (Fig. 3). Differences even extended among soils at each Zones, as Zone A and C had detectable peaks for calcite and kutnohorite and rhodochrosite, while Zone B and D did not (Fig. 3).

Due to the heterogeneity of minerals present in the soil (Fig. 3), particularly Mn-rich ones, total Mn concentrations exhibited a large variation for Ca, Mn, and Fe in soils derived from the mine spoils (Tables 3, 4). The average total Mn soil concentrations at the control sites were $980 \mu\text{g g}^{-1}$ (Table 4), which is within typical soil Mn concentrations of 100 to $4000 \mu\text{g g}^{-1}$ (Adriano 2001; Navrátil et al. 2007). However, soils at mine spoils Zones A through D were well-above typical soil concentrations as average total Mn concentrations were $5580 \mu\text{g g}^{-1}$ (Table 4). As expected, total Mn concentrations in the mine spoil soils were significantly greater than at control sites (Fig. 4). These total Mn concentrations did not exhibit a strong vertical pattern with depth (Table 4). Unlike Mn, total Ca soil concentrations were similar among the mine spoils, Zones B through D, and with both control sites ($p > 0.05$) (Fig. 4). Total and extractable Mn concentrations were most likely higher in Zones A and C compared to Zones B and D due to the abundance of rhodochrosite, calcite and kutnohorite, and rhodonite (Fig. 3).

We measured the nonsilicate, potentially plant available fraction, using a strong acid digestion to

capture Mn present in organic complexes and secondary oxides potentially accessible by roots and fungi (Wong 2003; Maiz et al. 2000). Overall Zones A through D had 10 times higher strong acid extractable Mn ($41 \mu\text{g g}^{-1}$) and Ca ($130 \mu\text{g g}^{-1}$) concentrations than the two control sites (Mn $5 \mu\text{g g}^{-1}$, Ca $7 \mu\text{g g}^{-1}$) ($p < 0.05$) (Fig. 4). Strong acid extractable Mn and Ca concentrations strongly varied with depth. The A horizons at Zones A through D, which approximately corresponds with 0 to 16 cm depth, had significantly higher strong acid extractable Ca and Mn than BC horizons at 54 to 80 cm depth ($p < 0.05$) (Table 3). Surface soils can have higher extractable Mn due to weathering of minerals by organic acids and plant roots (Navrátil et al. 2007; Herndon et al. 2019). When considering extractable concentrations as a percentage of their respective totals, strong acid extractable Mn at Zones A through D ($\sim 0.8\%$) were not significantly different compared with control sites ($\sim 0.5\%$) (Table 3). More importantly, strong acid extractable Ca was > 10 times higher at Zones A through D ($\sim 1.5\%$) compared with control sites ($\sim 0.1\%$). We conclude that the bulk portion of Mn remained in non-available silicate phases (rhodonite, spessartine, and other aluminosilicate minerals) and not in potentially plant available forms (organic-bound or secondary complexes readily dissolved by strong acids) or acid-soluble minerals like rhodochrosite or kutnohorite.

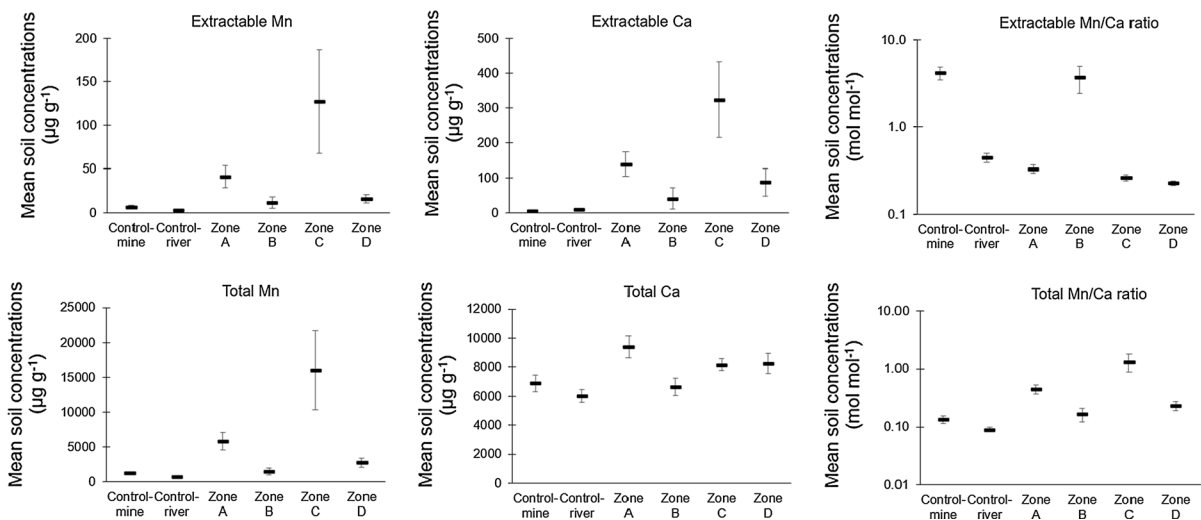


Fig. 4 Mean soil concentrations of total and extractable Mn and Ca across all soil horizons and soil pits at each mine spoil and control site. Error bars are ± 1 standard error

Foliar Ca, Mg, and Fe concentrations

Contrary to our original hypothesis, overall foliar Mn concentrations on the mine spoils, Zones A through D, were significantly lower than at the control mine and partially for control river sites ($p < 0.05$) (Fig. 5). When combined mine spoils ($840 \pm 141 \mu\text{g g}^{-1}$) were significantly lower than at the two control sites ($1667 \pm 337 \mu\text{g g}^{-1}$) ($p < 0.05$). Furthermore, overall foliar Ca concentrations were higher on the mine spoils ($5238 \pm 601 \mu\text{g g}^{-1}$) than at the two control sites ($2584 \pm 512 \mu\text{g g}^{-1}$) ($p < 0.05$) (Fig. 5). Due to these differences, Mn/Ca ratios were significantly lower for plants on the mine spoils ($0.25 \pm 0.07 \text{ mol mol}^{-1}$) than at the control sites ($1.13 \pm 0.28 \text{ mol mol}^{-1}$) ($p < 0.05$) (Fig. 5). These results refute our original hypothesis that trees growing on the Mn-rich mine spoils would have higher Mn concentrations than plants growing in surrounding soils, not impacted by mine spoils.

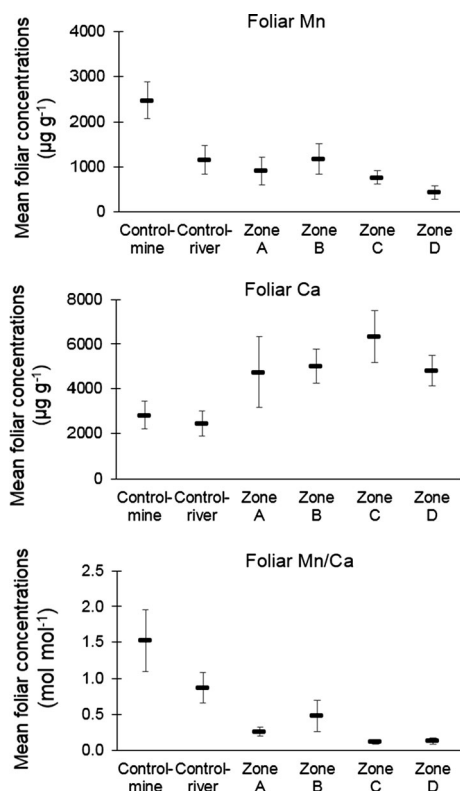


Fig. 5 Foliar Mn and Ca concentrations across all vegetation at each mine spoil and control site. Error bars are ± 1 standard error

Manganese concentrations in foliage on the mine spoils were in the potentially toxic concentration range; Mn toxicity in herbaceous plants has been observed to begin in foliar concentrations between 600 to 1250 $\mu\text{g g}^{-1}$ (Millaleo et al. 2010; Adriano 2001). However, toxicity did not appear to be important as the trees appeared to be healthy. Mid-summer leaves were without chlorosis or leaf-edge damage or senescence. Further, average DBH values for *Betula spp.*, *Fagus grandifolia*, and *Acer saccharum* were > 20 cm, which are typical values for growth rates in Massachusetts (Teck and Hilt 1991). We hypothesized the elevated Mn concentrations in the foliage did not lead to sustained Mn toxicity due to abundance of Ca. Mn-induced phytotoxicity can be mediated through accumulation of metals that Mn negatively impact, particularly Ca (Robson and Loneragan 1970). Thus, the soils derived from mine spoils have enough biologically available Ca to make up for elevated concentrations of extractable Mn, which were only a small fraction $< 1\%$ of the total Mn. For example, Clair and Lynch (2005) demonstrated that *Acer saccharum* is sensitive to Mn uptake and excess uptake can lead to impairment of photosynthesis and related metabolic processes. Moreover, lower Mn/Ca ratios occur in plant foliage that are less perturbed by anthropogenic forcings such as smelting or coal combustion (Herdon et al. 2010; Richardson 2017).

Although there were general trends across sites, there were important differences among genera and ecophysiological groups. First, significant differences for *Betula spp.*, *Fagus grandifolia*, and *Acer saccharum* had higher Mn concentrations and Mn/Ca ratios at control sites than on the mine spoils (Fig. 6). However, understory plants did not have significantly different Mn concentrations at control sites than mine spoil sites (Fig. 6). In addition, there were significant differences among tree species. *Acer pensylvanicum* and *Betula spp.* had the highest foliar Mn concentrations while *Fraxinus pennsylvanica* had the lowest foliar Mn concentrations of canopy trees when only considering the mine spoil Zones A through D (Fig. 6). This coincides with existing knowledge of trees of the genus *Betula*, are known to accumulate metals in their woody tissues at higher concentrations than other northern hardwood genera (e.g., Wisłocka et al. 2006). Considering Ca, however, *Betula spp.* had the lowest foliar Ca concentrations while *Fraxinus pennsylvanica* had the highest of the canopy trees on

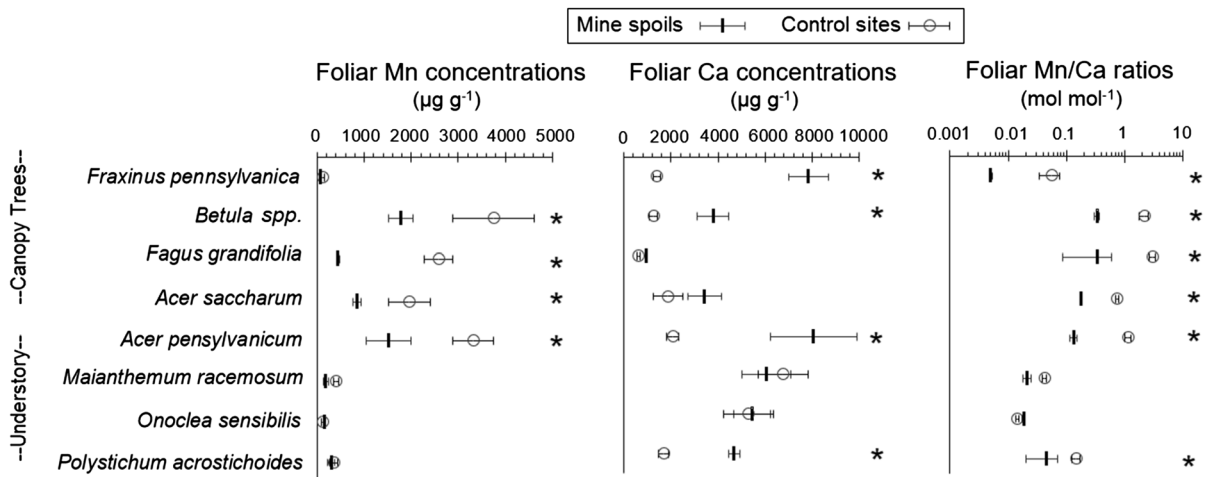


Fig. 6 Mean foliar Mn and Ca concentrations and molar Mn/Ca ratio for vegetation at the mine spoils Zones A, B, C, and D and the two control sites. Asterisk indicates a significant difference

mine spoil (Fig. 6). The lower uptake of Ca further demonstrates that metal ion uptake specificity varies strongly among trees. Further evidence supporting species dependent ion uptake specificity is that *Fagus grandifolia* had much lower foliar Mn and Ca concentrations than *Betula* spp. (Fig. 6).

Biogeochemistry of Mn in the mine spoil soils

The paradoxical lower Mn concentrations in foliage on mine spoils compared to control sites in spite of elevated total and strong acid extractable soil Mn concentrations can be explained by the biogeochemistry of Mn. Manganese is most soluble under reducing conditions and $\text{pH} < 6$ (Navrátil et al. 2007) while the forest soils in our study were strongly acidic but were well-oxidized. Our measured soil pH was significantly lower in soil horizons at control sites ($\text{pH} 4.2 \pm 0.4$) compared to mine spoils ($\text{pH} 5.1 \pm 0.3$) ($p < 0.05$; Table 2). Although soil oxidizing conditions were not directly measured throughout the year, we can assume they are not flooded due to the sandy soil texture ($> 72\%$ sand), no underlying restricting layer (e.g., fragipan, duripan), excessively well-drained class, and no redoximorphic feature present in the upper 1 m. We can assume only minimal fluctuations in the redox conditions during partial melting in the early winter and early spring (< 14 days) (Veneman et al. 1998). Thus, the pH and reduction potential of the soils were in the range to promote Mn precipitation as secondary

between mine spoils and control sites for a species or genus. Error bars are ± 1 standard error

oxides and we detected birnessite in A horizon XRD patterns in Zones A and D but not in the control sites.

Conclusions

We conclude that foliar Mn concentrations were not directly controlled by total or extractable soil Mn concentrations, but rather other geochemical properties that regulate bioavailability and uptake by plants including species-specific Mn and Ca uptake. First, most of the Mn was not extractable and thus not potentially plant available. Instead, Mn in the mine spoils likely remained in silicate (e.g., spessartine or rhodonite) and other residual phases in the soil profiles. Second, although the control sites have much lower total Mn in their rocks and minerals, the greater acidity, lower extractable Ca, and lower buffering capacity from weathering carbonates has likely caused greater Mn uptake at the control sites compared to the mine spoils. Third, two of the three herbaceous understory plants did not have contrasting foliar Mn concentrations or Mn/Ca ratios highlighting species dependency on Mn uptake. However, most woody plants had significantly higher Mn concentrations and Mn/Ca ratios when combining data from all four mine spoils zones and comparing with the combined control sites data. Lastly, our foliar results show that the northern hardwood forests established on mine spoils at the Betts Mine had lower foliar Mn concentrations

and Mn/Ca ratios than at an adjacent control site and also partially for a control site 2.3 km away, off of the Hawley formation, refuting our initial hypothesis. The potential impact of Mn accumulation and toxicity on plants was dependent on genera and ecophysiology (canopy compared to understory plants). These results suggest Mn toxicity on mine soils and tailings may be overcome through ensuring a higher soil pH and abundance of potentially plant available Ca.

Acknowledgements We are indebted to John Fellows for suggesting the study location and Bruce Hooke and Earthdance Creative Living Project, Inc. for generously giving their permission to study the former Betts Mine. We are thankful for field assistance from Rudolph Marek the IV and Brendan Braithwaite with collecting upper canopy branches and soil pit excavation, respectively. In addition, we are thankful for laboratory assistance from Hamid Mashayekhi and Nicholas Martone for ICP-MS analyses and XRF analyses, respectively. This research was supported by funding to Dr. Justin Richardson from the University of Massachusetts Amherst.

References

- Adriano, D. C. (2001). Arsenic. In *Trace elements in terrestrial environments* (pp. 219–261). Springer, New York.
- Chen, M., & Ma, L. Q. (1998). Comparison of four USEPA digestion methods for trace metal analysis using certified and Florida soils. *Journal of Environmental Quality*, 27, 1294–1300.
- Clair, S. B., & Lynch, J. P. (2005). Element accumulation patterns of deciduous and evergreen tree seedlings on acid soils: Implications for sensitivity to manganese toxicity. *Tree Physiology*, 25, 85–92.
- Da Silva, J. F., & Williams, R. J. P. (2001). *The biological chemistry of the elements: The inorganic chemistry of life*. Oxford: Oxford University Press.
- Grazulis, S., Chateigner, D., Downs, R. T., Yokochi, A. F. T., Quiros, M., Lutterotti, L., et al. (2009). Crystallography open database—An open-access collection of crystal structures. *Journal of Applied Crystallography*, 42, 726–729.
- Gee, G. W., & Bauder, J. W. (1985). *Methods of analysis for soils, plants and water*. Univ. of Calif, Div. of Agril. Sci., California, USA, pp. 123–125.
- Herndon, E. M., Jin, L., & Brantley, S. L. (2010). Soils reveal widespread manganese enrichment from industrial inputs. *Environmental Science and Technology*, 45, 241–247.
- Herndon, E., Yarger, B., Frederick, H., & Singer, D. (2019). Iron and manganese biogeochemistry in forested coal mine spoil. *Soil Systems*, 3(1), 13.
- Hickmott, D. D. (1982). The mineralogy and petrology of the Betts mine area, Plainfield, Massachusetts. *Unpublished B.S. thesis* (p. 105). Amherst: Amherst College.
- Hickmott, D. D., Slack, J. F., & Docka, J. A. (1983). Mineralogy, petrology, and genesis of manganese ores of the Betts Mine, Hampshire County, Massachusetts. In D. F. Sangster (Eds.) *Field trip guidebook to stratabound sulphide deposits, Bathurst Area, N.B., Canada and West-Central New England, U.S.A.*
- Juárez-Santillán, L. F., Lucho-Constantino, C. A., Vázquez-Rodríguez, G. A., Cerón-Ubilla, N. M., & Beltrán-Hernández, R. I. (2010). Manganese accumulation in plants of the mining zone of Hidalgo, Mexico. *Bioresource Technology*, 101, 5836–5841.
- Kabata-Pendias, A., & Mukherjee, A. B. (2007). *Trace elements from soil to human*. Berlin: Springer.
- Kraepiel, A. M. L., Dere, A. L., Herndon, E. M., & Brantley, S. L. (2015). Natural and anthropogenic processes contributing to metal enrichment in surface soils of central Pennsylvania. *Biogeochemistry*, 123, 265–283.
- Krauskopf, K. B. (1979). *Introduction to geochemistry. International series in the earth and planetary sciences*. Tokyo: Mc Grow-Hill.
- Kreutzer, K. (1972). The effect of Mn deficiency on colour, pigment and gas exchange of Norway spruce needles. *Forstwissenschaftliches Centralblatt*, 91(2), 80–89.
- Li, M. S., Luo, Y. P., & Su, Z. Y. (2007). Heavy metal concentrations in soils and plant accumulation in a restored manganese mineland in Guangxi, South China. *Environmental Pollution*, 147, 168–175.
- Li, M. S., & Yang, S. X. (2008). Heavy metal contamination in soils and phytoaccumulation in a manganese mine wasteland, South China. *Air, Soil and Water Research*, 1 ASWR-S2041.
- Lilliefors, H. W. (1967). On the Kolmogorov–Smirnov test for normality with mean and variance unknown. *Journal of the American statistical Association*, 62, 399–402.
- Maiz, I., Arambarri, I., Garcia, R., & Millan, E. (2000). Evaluation of heavy metal availability in polluted soils by two sequential extraction procedures using factor analysis. *Environmental Pollution*, 110, 3–9.
- Millaleo, R., Reyes-Díaz, M., Ivanov, A. G., Mora, M. L., & Alberdi, M. (2010). Manganese as essential and toxic element for plants: Transport, accumulation and resistance mechanisms. *Journal of soil science and plant nutrition*, 10, 470–481.
- Navrátil, T., Shanley, J. B., Skřivan, P., Krám, P., Mihaljevič, M., & Drahota, P. (2007). Manganese biogeochemistry in a central Czech Republic catchment. *Water, Air, and Soil Pollution*, 186(1–4), 149–165.
- Pollard, A. J., Stewart, H. L., & Roberson, C. B. (2009). Manganese hyperaccumulation in *Phytolacca americana* L. from the Southeastern United States. *Northeastern Naturalist*, 16(sp5), 155–163.
- Quinn, A. W. (1945). *Geology of the Plainfield-Hawley area, Massachusetts (with special reference to deposits of manganese and iron minerals): Massachusetts Department of Public Works. United States Geological Survey Cooperative Geology Project, Open-File Report* (p. 38).
- Richardson, J. B. (2017). Manganese and Mn/Ca ratios in soil and vegetation in forests across the northeastern US: Insights on spatial Mn enrichment. *Science of the Total Environment*, 581, 612–620.
- Richardson, J. B., & Friedland, A. J. (2016). Influence of coniferous and deciduous vegetation on major and trace

- metals in forests of northern New England, USA. *Plant and Soil*, 402, 363–378.
- Richardson, J. B., Friedland, A. J., Engerbretson, T. R., Kaste, J. M., & Jackson, B. P. (2013). Spatial and vertical distribution of mercury in upland forest soils across the northeastern United States. *Environmental Pollution*, 182, 127–134.
- Robson, A. D., & Loneragan, J. F. (1970). Sensitivity of annual Medicago species to manganese toxicity as affected by calcium and pH. *Australian Journal of Agricultural Research*, 21, 223–232.
- Santisteban, J. I., Mediavilla, R., Lopez-Pamo, E., Dabrio, C. J., Zapata, M. B. R., García, M. J. G., et al. (2004). Loss on ignition: A qualitative or quantitative method for organic matter and carbonate mineral content in sediments? *Journal of Paleolimnology*, 32(3), 287–299.
- Stubblefield, W. A., Brinkman, S. F., Davies, P. H., Garrison, T. D., Hockett, J. R., & McIntyre, M. W. (1997). Effects of water hardness on the toxicity of manganese to developing brown trout (*Salmo Trutta*). *Environmental Toxicology and Chemistry*, 16(10), 2082–2089.
- Teck, R. M., & Hilt, D. E. (1991). Individual-tree diameter growth model for the Northeastern United States. Research paper NE-649. Radnor, PA: U.S. Department of Agriculture, Forest Service, Northeastern Forest Experiment Station, 11 pg. Ter-Mikaelian M T, Korzukhin MD 1997 Biomass equations for sixty-five North American tree species. *Forest Ecology and Management*, 97, 1–24.
- Veneman, P. L. M., Spokas, L.A., & Lindbo, D. L. (1998). Soil moisture and redoximorphic features: A historical perspective. In M. C. Rabenhorst, J. C. Bell, & P. A. McDaniel (Eds.), *Quantifying soil hydromorphology* (pp. 1–23). Madison: Soil Science Society of America.
- Watmough, S. A., Eimers, M. C., & Dillon, P. J. (2007). Manganese cycling in central Ontario forests: Response to soil acidification. *Applied Geochemistry*, 22, 1241–1247.
- Westfall, L. A., Davourie, J., Ali, M., & McGough, D. (2016). Cradle-to-gate life cycle assessment of global manganese alloy production. *The International Journal of Life Cycle Assessment*, 21, 1573–1579.
- Wisłocka, M., Krawczyk, J., Klink, A., & Morrison, L. (2006). Bioaccumulation of heavy metals by selected plant species from uranium mining dumps in the Sudety Mts., Poland. *Polish Journal of Environmental Studies*, 15(5), 811–818.
- Wong, M. H. (2003). Ecological restoration of mine degraded soils, with emphasis on metal contaminated soils. *Chemosphere*, 50(6), 775–780.
- Xue, S. G., Chen, Y. X., Reeves, R. D., Baker, A. J., Lin, Q., & Fernando, D. R. (2004). Manganese uptake and accumulation by the hyperaccumulator plant *Phytolacca acinosa* Roxb. (Phytolaccaceae). *Environmental Pollution*, 131(3), 393–399.
- Yang, S., Liang, S., Yi, L., Xu, B., Cao, J., Guo, Y., et al. (2014). Heavy metal accumulation and phytostabilization potential of dominant plant species growing on manganese mine spoils. *Frontiers of Environmental Science & Engineering*, 8, 394–404.

Publisher's Note Springer Nature remains neutral with regard to jurisdictional claims in published maps and institutional affiliations.